

Optical validation and characterization of *Planck* PSZ2 sources at the Canary Islands observatories. II. Second year of LP15 observations

A. Aguado-Barahona^{1,2}, R. Barrena^{1,2}, A. Streblyanska^{1,2}, A. Ferragamo^{1,2}, J.A. Rubiño-Martín^{1,2}, D. Tramonte^{3,1,2}, and H. Lietzen⁴

(Affiliations can be found after the references)

ABSTRACT

Context. The second legacy catalogue of Planck Sunyaev-Zeldovich (SZ) sources, hereafter PSZ2, provides the largest galaxy cluster sample selected by means of their SZ signature in a full sky survey. In order to fully characterise this PSZ2 sample for cosmological studies, all the members should be validated and the physical properties of the clusters, including mass and redshift, should be derived. However, at the time of its publication roughly 21 per cent of the 1653 PSZ2 members had no known counterpart at other wavelengths.

Aims. Here, we present the second and last year of observations of our optical follow-up programme 128-MULTIPLE-16/15B (hereafter LP15), which has been developed with the aim of validating all the unidentified PSZ2 sources in the northern sky, with declination above -15° , and with no correspondence in the first Planck catalogue PSZ1. The description of the programme and the first year of observations were presented in Streblyanska et al. (2019).

Methods. The LP15 programme was awarded 44 observing nights, spread over two years in the Isaac Newton Telescope (INT), the Telescopio Nazionale Galileo (TNG) and the Gran Telescopio Canarias (GTC), all at Roque de los Muchachos Observatory (La Palma). Following the same methodology described in Streblyanska et al. (2019), at the end of the LP15 programme we performed deep optical imaging for more than 200 sources with the INT, and spectroscopy for almost 100 sources with the TNG and GTC. We adopted a robust confirmation criteria based on velocity dispersion and richness estimations in order to carry out the final classification of the new galaxy clusters as the optical counterparts of the PSZ2 detections.

Results. Here, we present the observations of the second year of LP15, as well as the final results of the programme. The full LP15 sample comprises 190 previously unidentified PSZ2 sources. Of those, 106 objects were studied in Streblyanska et al. (2019), while the remaining sample (except for 6 candidates) has been completed in the second year and it is discussed here. In addition to the LP15 sample, in this paper we have studied 42 additional PSZ2 objects, which were originally validated as real clusters due to their matching with a WISE or PSZ1 counterpart, but they had no measured spectroscopic redshift. In total, we have confirmed the optical counterpart for 81 PSZ2 sources after the full LP15 programme, 55 of them with new spectroscopic information. Out of those 81 sources, 40 clusters are presented in this paper. After the LP15 observational programme the purity of the PSZ2 catalogue has increased from 76.7 % originally to 86.2 %. In addition, we study the possible reasons of having false detection, and we report a clear correlation between the number of unconfirmed sources and galactic thermal dust emission.

Key words. large-scale structure of Universe – Galaxies: clusters: general – Catalogues

1. Introduction

Galaxy Clusters (GCs) are a very powerful tool to test the cosmological model (Allen et al. 2011). They have been used for cosmology studies since Zwicky's discovery of dark matter in the Coma Cluster (Zwicky 1933), and thanks to the recent all-sky surveys appearing during the last decade, their study has increased significantly. In particular, the *Planck*¹ satellite (Planck Collaboration I 2014) provided for the first time the possibility for the detection of GCs on a full-sky survey by means of the Sunyaev-Zeldovich (SZ) effect (Sunyaev & Zeldovich 1972), which is Cosmic Microwave Background (CMB) spectral distortion. As CMB photons go through a GC, they can interact with the hot intra-cluster medium (ICM) electrons via inverse Compton scattering. As a result of this interaction, the CMB photons gain energy and the overall CMB spectrum is shifted

towards higher frequencies, producing a characteristic spectral dependence which can be used for their detection.

In order to use the GCs surveys to constrain cosmological parameters (Planck Collaboration VI 2018; Planck Collaboration XXIV 2016), it is important to obtain unbiased measurements of the cluster mass and redshift. In particular, due to the fact that the surface brightness of the SZ effect does not depend on redshift, follow-up campaigns at other wavelengths are needed in order to complement the SZ information. The detailed characterisation of *Planck* SZ survey cluster sample is needed to improve cosmological constraints from *Planck* survey alone, and also to obtain constraints from future large galaxy cluster surveys, e.g. SRG/eROSITA cluster survey (Predehl et al. 2010), whose spacecraft was successfully launched on July 13th and the first light of SRG/eROSITA telescope is planned to be obtained very soon.

The PSZ2 catalogue (Planck Collaboration XXVII 2016) is the second *Planck* catalogue of Sunyaev-Zeldovich sources derived from the full 29 months mission data. This catalogue is based on the results from three cluster detection codes (MMF1, MMF3 and PwS) described in detail in Planck Collaboration

¹ *Planck* <http://www.esa.int/Planck> is a project of the European Space Agency (ESA) with instruments provided by two scientific consortia funded by ESA member states and led by Principal Investigators from France and Italy, telescope reflectors provided through a collaboration between ESA and a scientific consortium led and funded by Denmark, and additional contributions from NASA (USA).

XXIX (2014); Planck Collaboration XXVII (2016). The PSZ2 was validated using external X-ray, optical, SZ and near-IR data and contained, at the time of its publication, 1653 detections of which 1203 were confirmed as actual galaxy clusters, 1094 of them including redshifts. The PSZ2 catalogue contains all objects found by at least one of the three detection algorithms with $S/N \geq 4.5$ for the SZ detection.

A first validation process was performed in Planck Collaboration XXVII (2016). It began using a cross-match with the PSZ1, continuing the search for possible counterparts in the MCXC catalogue (Piffaretti et al. 2011) which is based on the *ROSAT* All Sky Survey (RASS, Voges et al. 1999, 2000) and on the serendipitous *ROSAT* and Einstein cluster catalogues, in the Sloan Digital Sky Survey (SDSS York et al. 2000), in the redMaPPer catalogue (Rykoff et al. 2014), in NED² in similar follow-ups (Planck Collaboration int. XXVI 2015; Planck Collaboration int. XXXVI 2016) as the one presented in this work, in the ALLWISE mid-infrared source catalogue (Cutri et al. 2013) as well as in SZ catalogues such as the catalogues obtained by the South Pole Telescope (SPT, Bleem et al. 2015), by the Atacama Cosmology Telescope (ACT, Hasselfield et al. 2013) and by direct follow-up with the Arc-minute Micro-kelvin Interferometre (AMI, Perrott et al. 2015).

This paper is the last of a series of papers where optical characterisation of SZ sources was performed using the Canary Islands Observatories. Planck Collaboration int. XXXVI (2016); Barrena et al. (2018) study PSZ1 sources thanks to the observational programme ITP13-08. Later, a second long-time programme was granted 128-MULTIPLE-16/15B (hereafter LP15) to study the PSZ2 sources. Streblyanska et al. (2019, hereafter Paper I) and this paper are the result of this last programme. The main motivation of these follow-up campaigns is to identify and confirm optical cluster counterparts of unknown sources. We perform photometric and spectroscopic observations in order to study the optical richness and estimate velocity dispersion. We leave the mass estimates for future works.

This paper is structured as follows. Sections 2 and 3 describe the observational programme carried out for this work, including the instrumentation setups, the observational approach as well as the criteria used to validate candidates as optical counterparts for SZ sources. Section 4 presents the observations for the 2nd year of this programme and details some special cases. In Section 5 we update information about already known counterpart validated using ALLWISE (Cutri et al. 2013). Section 6 summarises the whole programme and gives the final results for this work. Section 7 presents the conclusions.

We adopt Λ CDM cosmology with $\Omega_m = 0.3075$, $\Omega_\Lambda = 0.691$ and $H_0 = 67.74 \text{ km s}^{-1} \text{ Mpc}^{-1}$.

2. LP15 optical follow-up campaign

2.1. Sample definition and observational strategy

The LP15 programme, the sample definition and the observing strategy are described in detail in paper I. Here, we briefly summarise its basic characteristics and present the second year of observations. As a reminder, the main motivation of the programme is to carry out a systematic follow-up of the complete set of PSZ2 cluster candidates in the northern sky, with no confirmed counterparts at the moment of the catalogue publication. For LP15,

we consider only sources located at declination $> -15^\circ$. As a reference, the full PSZ2 catalogue contains a total set of 1003 sources in that region.

The LP15 sample is defined by all those sources in PSZ2 with declination above -15° , which also have $\text{validation} = -1$ (i.e., no known counterpart at the time of the publication of the catalogue), and $\text{PSZ1} = -1$ (i.e. no matching detection in the PSZ1). This corresponds to 190 targets in total, 106 of which were already discussed in paper I.

During the second year of the programme, covering the semesters 2016B and 2017A, we continued with the observations of the remaining LP15 sample. As for the previous year, the second year of observations were carried out at the Roque de los Muchachos Observatory (ORM) located at La Palma island (Spain) between August 2016 and August 2017. The three telescopes used in this work are: a) the 2.5 m Isaac Newton Telescope (INT) operated by the Isaac Newton Group of Telescopes; b) the 3.6 m Italian Telescopio Nazionale Galileo (TNG) operated by the Galileo Galilei Foundation of the INAF (Istituto Nazionale di Astrofisica); and c) the 10.4 m Gran Telescopio Canarias (GTC) operated by the Instituto de Astrofísica de Canarias (IAC). More information about their instruments and technical features were presented in Table 1 of Paper I, as well as information about the observing nights and the number of candidates observed.

Our follow-up programme is structured as follows. The first step is to select a target for deep-imaging observations and if galaxy over-densities are found, confirm the cluster using spectroscopy. The photometric observations are carried out in the INT using three broadband Sloan filters (g' , r' , i'). Based on colour combinations of these filters, we are able to estimate photometric redshifts (Planck Collaboration int. XXXVI 2016) of possible members of the cluster up to $z \sim 0.8$. In the second step, candidates are definitely confirmed using multi-object spectroscopy (MOS) either in the TNG or in GTC, depending on the photometric estimation of the redshift of the candidate. Due to the greater collecting area of the GTC, we use it for distant clusters ($z > 0.35$), while the TNG for the closest ones ($z < 0.35$). The final step is to validate the candidates using the confirmation criteria explained in Sect. 3.

2.2. Imaging and spectroscopic observation and data reduction

The complete technical description of the telescopes and instrument set-ups used during LP15 programme and information on corresponding data reduction is detailed in Paper I. Here, we briefly summarise the information of the imaging and spectroscopic observations and data reduction performed during the second year of the programme.

Optical observations were carried out during multiple runs between August 2016 and August 2017. Deep images were obtained using the Wide-Field Camera (WFC) installed in the 2.5 m in INT. Spectroscopic observations were obtained using the multi-object spectrographs DOLORES@TNG and OSIRIS@GTC. The spectroscopic data from DOLORES was retrieved during multiple runs between November 2016 and August 2017 and the data from OSIRIS was acquired in service mode between September 2016 and August 2017.

All images and spectra were reduced using IRAF³ standard routines. The astrometry was performed using the

² The NASA/IPAC Extragalactic Database (NED) is operated by the Jet Propulsion Laboratory, California Institute of Technology, under contract with the National Aeronautics and Space Administration

³ IRAF (<http://iraf.noao.edu/>) is distributed by the National Optical Astronomy Observatories, which are operated by the Association

images.imcoords task and the USNO B1.0 catalogue (Monet et al. 2003) as reference obtaining a final accuracy of $rms \sim 0.2''$ across the full field of view. The photometric calibration is referred to SDSS photometry. In the case of fields with SDSS coverage, we performed the direct cross-correlation with the SDSS photometric data. Using SExtractor (Bertin & Arnouts 1996) programme in single-image mode, we created individual source catalogues for each band. All catalogues were then merged in the final one with a search radius of $1''$.

Standard spectroscopic data reduction included sky subtraction, extraction of spectra, cosmic rays rejection, and wavelength calibration (using specific arcs). Our final reduced spectra have typical $S/N \sim 5$ per pixel (at around 6000 \AA) for galaxies with magnitudes $r' \sim 20.5$ and 21.7 observed with the TNG and GTC, respectively.

We estimated radial velocities using task RVSAO⁴. Figure 1 shows two examples of spectra for low and high- z galaxies obtained at the TNG and GTC. Thanks to the capabilities of the MOS observations, we were able to retrieve typically 20 members per cluster with which to estimate the mean redshift and velocity dispersion of the systems. The cluster redshift is taken to be the mean value of the galaxy members retrieved. The galaxies are considered members only if they showed radial velocities of $\pm 2500 \text{ km s}^{-1}$ in rest frame with respect to the mean velocity of the system. Then, we follow an iterative method considering galaxies as members if their radial velocity is less than 2.5 times the velocity dispersion away from the cluster mean velocity. We follow this procedure in order to minimise the contamination of interlopers. The velocity dispersion and mass of the clusters will be published in a future work.

The broad band images used to carry out this work has been already included in the Virtual Observatory (VO) collection for public access. In the near future, the photometric and spectroscopic catalogues will be also available through this platform.

3. Cluster identification and validation criteria

Here we describe the methodology used to validate a cluster candidate as the optical counterpart of a PSZ2 target. This procedure is similar to the one adopted in paper I, and it is an extension of the methodology applied in Planck Collaboration int. XXXVI (2016); Barrena et al. (2018). Compared to other methods in the literature, we have improved the validation criteria by including visual inspection and comparison between the RGB images, and also the Compton y -maps (Planck Collaboration XXII 2016), making photometric redshift estimates and analysing the red sequence (hereafter RS Gladders & Yee 2000) using colour-magnitude diagrams. We have also performed a richness study considering galaxy counts in clusters. For approximately 30 % of our sample we have performed spectroscopic confirmation by estimating the velocity dispersion of the candidates.

3.1. Photometric analysis

The first step in our validation process is to visually inspect the deep RGB images and compare them with the Compton y -map of the SZ source. Having as reference the nominal *Planck* pointing coordinates, we look for galaxy over-densities around $5'$ radius, which is 2.5 times the *Planck* mean position error (Planck

Collaboration XXVII 2016). However, for a few cases, when a possible counterpart is found further than $5'$, we perform a more detailed analysis. It must be clear that in this first step we identify galaxy over-densities in the field of view but not everyone of them is associated with the SZ source. The next steps are performed in order to study this possible association.

We use colour-magnitude diagrams to identify likely cluster members and fit the RS to make an estimate of the photometric redshift using the methodology explained in Barrena et al. (2018), Sect. 3 and in Planck Collaboration int. XXXVI (2016), Sect. 4.2. To do so, we use $(g' - r')$ and $(r' - i')$ colours and consider galaxies within ± 0.05 from the Brightest Cluster Galaxy (BCG) colour.

The SZ clusters of the *Planck* catalogue are expected to be massive structures ($\gtrsim 5 \times 10^{14} M_{\odot}$) (see Planck Collaboration XXIX 2014) and therefore, they should present rich galaxy cluster populations. In order to discard the low mass systems from the real massive counterparts, we define a richness parameter (R_0) and its significance above the background level σ_R . The detailed description of our richness calculations is given in Paper I. Briefly, for a given cluster, we count likely cluster members (assumed as galaxies within the RS ± 0.15 , in colour) showing r' -magnitudes in the range $[m_{r'}^* - 1, m_{r'}^* + 1.5]$ within the 1 Mpc from the cluster centre. For this task, we consider as a BCG the most luminous galaxy of the identified likely cluster members. In order to obtain the background subtracted richness and decontaminate from the galaxy field contribution, we compute galaxy counts outside the 1 Mpc region and using the same restrictions in colour and magnitude as explained before, thereby creating a field galaxy sample or local background for each cluster (R_f). This field sample is scaled to the 1 Mpc area and subtracted from the cluster counts to obtain a statistical estimate of the number of galaxies for each cluster, the so-called richness ($R_{cor} \equiv R_0 - R_f$). We based our confirmation on the significance above the background level σ_R which is computed as $R_{cor} / \sqrt{R_f}$. For a better understanding see Fig. 2 which shows galaxy counts as a function of redshift in the field of the confirmed cluster PSZ2 G032.31+66.07. The initial value found for this cluster was $R_0 = 20.0$, and for the field at the redshift of the cluster was $R_f = 6.4$, yielding to $R_{cor} = 13.6$ and $\sigma_R = 5.4$.

3.2. Spectroscopic analysis

We performed spectroscopic observations for approximately 30 % of our sample, and include public data from the SDSS spectroscopic archive. We built radial velocity catalogues for each cluster and obtained the velocity dispersion in order to distinguish between poor and massive systems.

Planck systems must have masses $M_{500} \gtrsim 10^{14} M_{\odot}$ at low redshift ($z < 0.2$) and $M_{500} \gtrsim 2 \times 10^{14} M_{\odot}$ at higher redshift (see van der Burg et al. 2016, Fig.4). Using the scaling relations $M_{500} - \sigma_v$ from Munari et al. (2013) and $M_{500} - M_{200}$ from Komatsu et al. (2011), those values of mass lead to a velocity dispersion of $\sigma_v > 500 \text{ km s}^{-1}$ for $z < 0.2$ and $\sigma_v > 650 \text{ km s}^{-1}$ for $z \geq 0.2$. We adopt here the same criteria used in previous validation studies of *Planck* clusters (Planck Collaboration int. XXXVI 2016; Barrena et al. 2018; Streblyanska et al. 2019). The velocity dispersion of the candidates will be presented in a future work.

of Universities for Research in Astronomy, Inc., under the cooperative agreement with the National Science Foundation.

⁴ RVSAO was developed at the Smithsonian Astrophysical Observatory Telescope Data Center.

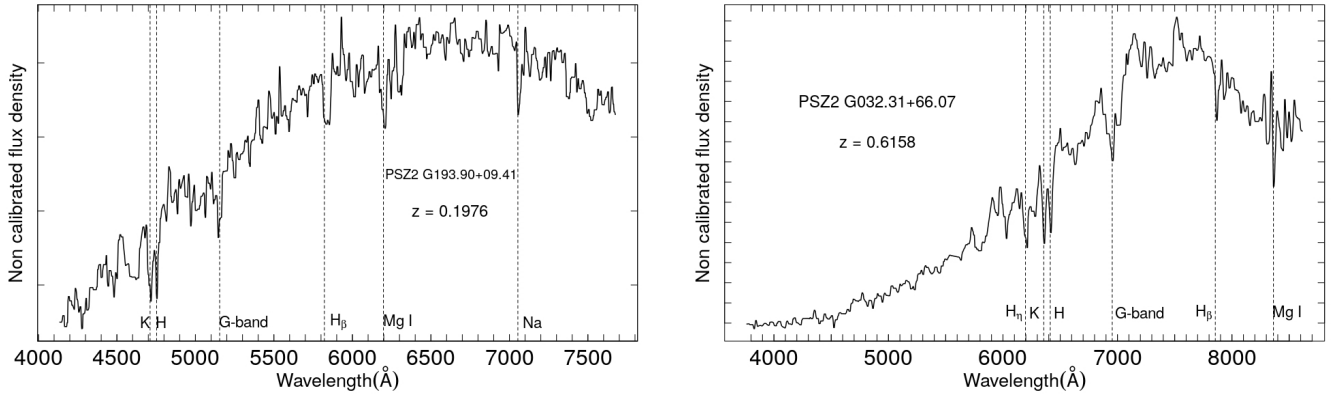


Fig. 1. Example of the spectra obtained with TNG/DOLORES (left panel) and GTC/OSIRIS (right panel) for two luminous galaxy members in the PSZ2 G193.90+09.41 and PSZ2 G032.31+66.07 clusters, at $z = 0.1976$ and $z = 0.6158$, respectively. Dashed lines correspond to the wavelength of the absorption features identified in each spectrum at the redshift of the clusters. Flux density is plotted in arbitrary units.

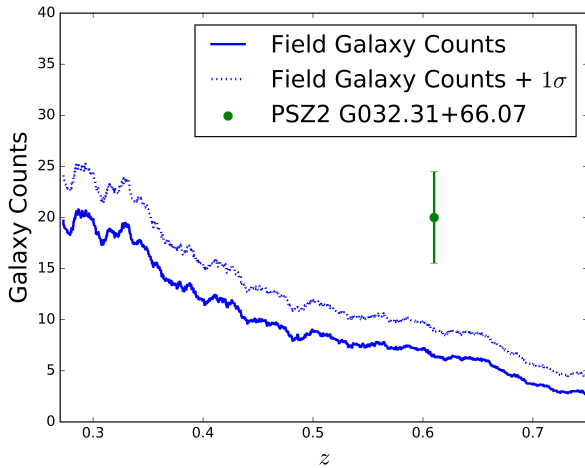


Fig. 2. Galaxy counts as a function of redshift in the field of the spectroscopically confirmed cluster PSZ2 G032.31+66.07. The galaxy counts for this particular cluster and its $1\text{-}\sigma$ error bars are shown in green. The blue line represents the galaxy counts outside 1 Mpc region from the optical centre of the cluster and the dashed blue line represents 1σ uncertainty above the latter.

3.3. Confirmation criteria adopted in this work

Table 1 summarises the set of criteria adopted in this work in order to confirm or reject a cluster candidate as the optical counterpart of the SZ signal. These are the very same criteria used in Paper I, and provide a classification of the candidates according to four possible values of a Flag. Values of Flag= 1 or 2 correspond to validated clusters; Flag= 3 corresponds to clusters located along the line of sight of the *Planck* signal but possibly not associated with the SZ emission; and ND refer to non-detection. For those cases where we have enough spectroscopic information to provide an estimate of σ_v , if that value is found to be above the corresponding threshold, we validate the candidate with Flag 1. However, if σ_v is below the threshold, we assume that the system has a low mass and it is probably not linked to the SZ emission, being the candidates classified as Flag 3. In the case that no spectroscopic information is available, or if we cannot estimate of the velocity dispersion due to an

Table 1. Validation criteria adopted to confirm or reject candidates associated to the SZ emission.

Flag	Spectroscopy	σ_v (km s $^{-1}$)	σ_R
1	YES	$> 500 \text{ km s}^{-1}$ ($z < 0.2$)	> 1.5
		$> 650 \text{ km s}^{-1}$ ($z > 0.2$)	> 1.5
2	NO	–	> 1.5
3	YES	$< 500 \text{ km s}^{-1}$ ($z < 0.2$)	> 1.5
	NO	–	< 1.5
ND	–	–	–

insufficient number of galaxy members (less than 5 members), we validate the candidates using the richness estimate. Systems showing a $\sigma_R > 1.5$ are validated photometrically, but waiting for a definitive spectroscopic confirmation. These systems are classified with Flag 2. Clusters with Flag 3 represent very poor systems ($\sigma_R < 1.5$) with no spectroscopic information. The ND (non-detection) flag is used for those SZ candidates where we found no galaxy over-density in the optical images. We also consider the criterion that a *Planck* cluster must be placed within $5'$ radius from the nominal pointing because it represents 2.5 times the mean position error with respect to the SZ peak emission. Nevertheless, this criterion can be modulated due to the wide range of uncertainties in the position error in the PSZ2 catalogue, and the different shapes of the y-maps. The cases that do not match the validation criteria but are positively confirmed will be discussed in Sect. 4.1.

4. LP15 sample: 2nd year of observations

Table 2 summarises the basic information of programme LP15 after the two years of observations, concerning the characterisation of the LP15 sample. The results for year one of the programme were already discussed in Paper I. Here, table 3 presents the results for 78 PSZ2 galaxy cluster candidates studied in this optical follow-up during the second and last year. The table is organised as follows. Columns 1, 2 and 3 are the official ID number, the *Planck* Name and the SZ signal-to-noise ratio, re-

Table 2. Summary information of the long-term LP15 programme. For each year of the programme, we show the total number of observed candidates (column 2), the total number of validated clusters (column 3), and the fraction of those with spectroscopic measurements (column 4). For completeness, columns 5–8 also include the classification of the candidates according to our validation criteria described in Table 1. Note that validated clusters (column 3) are those with flags 1 or 2. The full LP15 sample contained 190 candidates. Thus, there are still 6 additional objected to be studied (see text for details).

Year	Observed	val	spec	Flag 1	Flag 2	Flag 3	ND
1	106	41	34	31	10	8	57
2	78	40	22	18	22	6	32
TOTAL:	184	81	56	49	32	14	89

spectively, as they appear in the PSZ2 catalogue. Columns 4 and 5 are the J2000 coordinates of the BCG when present, otherwise geometrical centre of the cluster is provided. Column 6 is the distance between *Planck* and the optical centre reported in this work. Columns 7 and 8 present the spectroscopic information when available: the mean spectroscopic redshift of the cluster and/or the BCG, and the number of spectroscopic members retrieved. Columns 9, 10 and 11 provide the photometric information: the photometric redshift, the estimation of the richness and the value σ_R as explained in Sect. 3.1. Column 12 lists the cluster classification following the Flag system described in Sect. 3.3. Finally, column 13 is reserved for special comments or notes about the individual candidates.

Following the confirmation criteria explained in Sect. 3.3, we find that 37 of our candidates have a single optical counterpart, and one additional is classified as double detection. We classify a source as double detection when we find two or more overdensities around the SZ emission peak that might contribute to this emission. The ones validated with a single optical counterpart are classified as follows: 17 as Flag 1 and 22 as Flag 2. In addition, we find 32 non-detection, flagged as ND, and six systems not associated with the corresponding SZ source (Flag 3). This means a total of 38 PSZ2 sources remaining unconfirmed.

We have partially focused our work using SDSS DR12 data to confirm PSZ2 clusters classified by Streblyanska et al. (2018) as ‘potentially associated’ with the SZ emission. We have obtained the redshift and the velocity dispersion for six of the photometrically confirmed clusters and we have re-confirmed six clusters using our own deep INT imaging data classifying them as Flag 1 and 2, respectively. From the ‘potentially associated’ sub-sample of Streblyanska et al. (2018) we have confirmed five as Flag 1. Here, we invalidate the PSZ2 G328.96+71.97, confirmed by Streblyanska et al. (2018). New SDSS DR14 data reveals that the counterpart proposed by the authors is part of a larger system whose BCG is 34.6 away from the *Planck* SZ pointing. This system will be discussed in detail in Section 4.1.

Figure 3 represents the spatial distribution of the optical counterpart centre with respect to the nominal centre in the *Planck* PSZ2 catalogue for the clusters in our sample flagged as ‘1’, ‘2’ and ‘3’. The median of the offsets of the clusters validated is 3.10 which is in agreement with the median of the position error computed from the PSZ2 catalogue (2.43). The mean values are also in agreement (3.3 and 2.6) but they are more sensitive to cases which their position error is too high. We find 25 (35) clusters within 4.46 (6.38) representing the 68 % (95 %) of the confirmed clusters.

Figure 4 shows the cluster optical centre offsets relative to their *Planck* SZ position as a function of cluster redshift. Although the limit in distance is 5' (see Sect. 3), there are some confirmed sources that exceed that value due to different reasons such as the high position error in the PSZ2 catalogue or

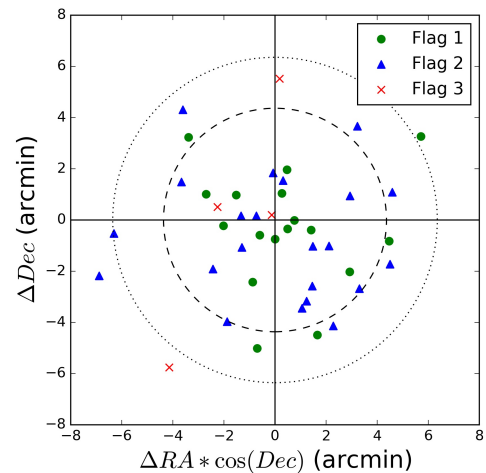


Fig. 3. Spatial distribution of the optical counterparts centres with respect to the nominal centre in the *Planck* PSZ2 catalogue. Green dots, blue triangles and red crosses correspond to clusters classified with Flag 1, Flag 2 and Flag 3, respectively. Dashed and dotted lines show the regions enclosing 68 % and 95 % of the confirmed clusters, flagged as ‘1’ and ‘2’, respectively

elongated y-map contour around the SZ emission peak (see Sect. 4.1).

Figure 5 presents a comparison between photometric and spectroscopic redshift estimations. Photometric redshifts were obtained as explained in Sect. 2. We show every observation carried out during the second year of the LP15, including the ones explained in Sect. 5. This study yields a mean photometric redshift error of $\delta z/(1+z) = 0.026$.

Finally, we note that there are six objects in the LP15 sample that have not been observed during the programme. One of them, PSZ2 G186.50–13.45, was already validated in Streblyanska et al. (2018), with a photometric redshift of $z_{\text{phot}} = 0.25$. According to our validation criterion, this case would correspond to a Flag= 2.

A dedicated proposal has been submitted and approved to complete the observations for the remaining five objects: PSZ2 G023.05+20.52, PSZ2 G092.34+14.22, PSZ2 G206.55–43.22, PSZ2 G210.37–37.00 and PSZ2 G247.14+25.88. These observations will be conducted in July 2019.

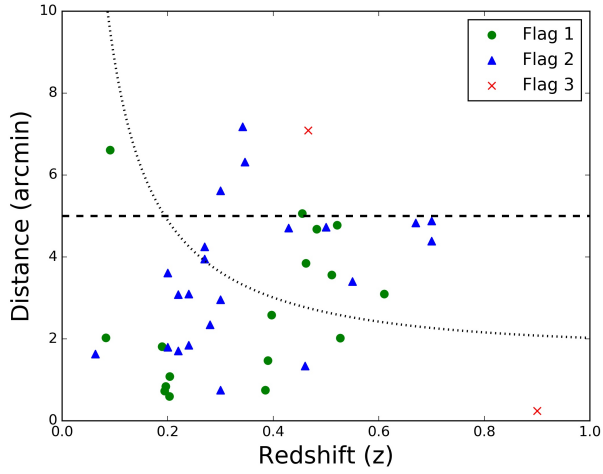


Fig. 4. Cluster optical centre offsets relative to their *Planck* SZ position as a function of cluster redshift. The dashed horizontal line at 5' shows the maximum offset expected for a *Planck* SZ detection. The dotted line corresponds to the angle subtended by 1 Mpc in projection at the corresponding redshift. Symbols used are the same as in Fig. 3.

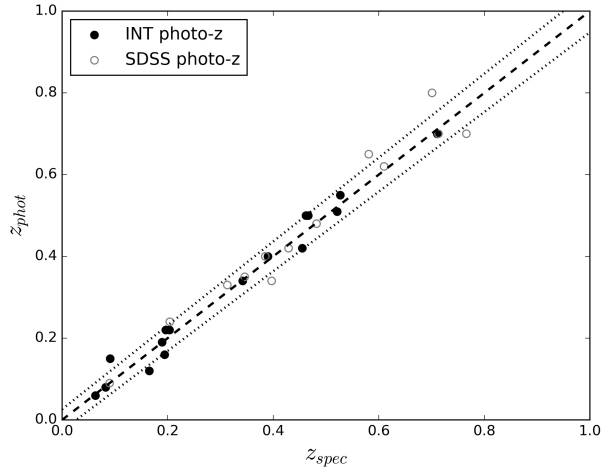


Fig. 5. Comparison between photometric and spectroscopic redshift estimations. Dashed line represents the 1:1 relation while dotted lines show the photometric redshift error $\delta z / (1 + z) = 0.026$.

Table 3. List of 78 PSZ2 cluster candidates analysed in this paper.

ID ¹	Planck Name	SZ SNR	Position (J2000)		Dist.(')	< z_{spec} > ; $z_{\text{spec,BCG}}$	N_{spec}	z_{phot}	R_{cor}	σ_R	Flag	Notes ²
			R. A.	Decl.								
115 ^{a,b}	PSZ2 G032.31+66.07	5.14	14 37 23.35	+24 24 21.70	3.10	0.610 ; –	38	0.62±0.05	13.6±3.7	5.4	1	(1), sub-structured
194	PSZ2 G048.47+34.86	5.74	–	–	–	–	–	–	–	–	ND	
242	PSZ2 G058.31+41.96	4.54	–	–	–	–	–	–	–	–	ND	
421-A ^c	PSZ2 G092.69+59.92	4.90	14 26 03.78	+51 14 18.50	3.85	0.462 ; 0.4568	25	0.50±0.05	11.6±3.4	4.3	1	(1,2)
421-B ^c			14 26 13.10	+51 11 53.17	4.42	0.844 ; –	5	–	–	–	3	(3)
424 ^b	PSZ2 G093.41–16.26	4.59	22 24 07.25	+37 58 30.46	3.10	–	–	0.24±0.03	40.6±6.4	7.9	2	WHL J222407.2+375831
432 ^{a,b}	PSZ2 G094.31–11.31	4.72	22 12 56.10	+42 35 46.34	1.08	0.204 ; –	27	0.24±0.03	–	–	1	
500	PSZ2 G104.52+39.39	4.60	15 58 38.88	+70 27 24.20	5.62	–	–	0.30±0.04	16.8±4.1	7.8	2	
511	PSZ2 G105.94–16.14	4.62	–	–	–	–	–	–	–	–	ND	
545	PSZ2 G112.54+59.53	5.37	–	–	–	–	–	–	–	–	ND	
546 ^c	PSZ2 G112.69+33.37	4.63	16 19 49.39	+79 06 24.49	4.78	0.521 ; 0.5194	15	0.51±0.03	–	–	1	(1), WHL J161949.3+790624
592	PSZ2 G120.75+25.39	4.69	–	–	–	–	–	–	–	–	ND	
600	PSZ2 G122.81+24.74	4.60	–	–	–	–	–	–	–	–	ND	
613	PSZ2 G125.25+33.33	5.38	11 41 11.26	+83 27 38.91	1.80	–	–	0.20±0.03	21.0±4.6	4.1	2	
616	PSZ2 G125.41+27.95	4.76	–	–	–	–	–	–	–	–	ND	
620 ^b	PSZ2 G125.84–18.72	5.30	01 06 55.65	+44 04 25.72	1.81	0.189 ; –	46	0.19±0.01	–	–	1	WHL J010709.2+440918
624 ^b	PSZ2 G126.36–19.11	5.01	01 09 19.57	+43 37 40.41	0.60	0.203 ; 0.2007	22	0.22±0.01	–	–	1	WHL J010919.5+433741
627	PSZ2 G126.62–53.42	4.55	–	–	–	–	–	–	–	–	ND	
628 ^b	PSZ2 G126.72–21.03	4.68	01 10 27.91	+41 40 57.27	0.84	0.196 ; –	9	0.22±0.03	–	–	1	WHL J011025.0+414119
640	PSZ2 G129.99–22.42	4.55	–	–	–	–	–	–	–	–	ND	
644-A ^b	PSZ2 G130.64+37.16	4.80	10 47 45.54	+77 59 56.67	2.82	0.473 ; 0.4722	14	0.44±0.03	16.7±4.1	5.0	1	WHL J104745.5+775957
644-B ^b			10 46 29.31	+78 07 44.06	6.07	–	–	0.24±0.02	49.3±7.0	11.9	2	(1), WHL J104629.2+780744
646 ^b	PSZ2 G131.15–14.72	5.37	01 38 42.22	+47 22 35.27	1.71	–	–	0.22±0.03	50.2±7.1	11.3	2	WHL J013846.1+472236
647	PSZ2 G131.19+14.48	4.80	–	–	–	–	–	–	–	–	ND	
648	PSZ2 G131.27–25.82	4.50	–	–	–	–	–	–	–	–	ND	
667 ^c	PSZ2 G136.02–47.15	4.64	01 28 23.61	+14 41 13.60	7.09	0.466 ; 0.4648	8	0.50±0.03	13.1±3.6	4.2	3	WHL J012823.6+144114
700	PSZ2 G143.90+25.06	4.91	–	–	–	–	–	–	–	–	ND	
712 ^a	PSZ2 G146.10–55.55	4.67	01 42 46.53	+04 59 48.72	4.71	0.429 ; –	1	0.42±0.04	10.8±3.3	3.0	2	
713	PSZ2 G146.13+40.97	4.90	09 40 17.10	+66 24 02.56	7.18	0.342 ; 0.3379	4	0.34±0.04	7.0±2.6	3.5	2	
717	PSZ2 G146.88+17.13	6.13	–	–	–	–	–	–	–	–	ND	
720	PSZ2 G147.17+42.67	4.92	09 50 01.152	+64 55 29.52	1.34	– ; 0.4401	1	0.46±0.04	7.4±2.7	3.1	2	(4)
727	PSZ2 G149.73+24.49	4.52	–	–	–	–	–	–	–	–	ND	
732 ^{a,b}	PSZ2 G150.64–14.21	4.68	03 17 04.20	+40 41 33.22	3.08	–	–	0.22±0.02	26.1±5.1	8.2	2	WHL J031704.2+404133
739 ^{a,c}	PSZ2 G152.40+75.00	4.70	12 13 19.17	+39 46 26.84	5.06	0.455 ; –	9	0.42±0.03	31.3±5.6	9.0	1	(1), WHL J121319.2+394627
740	PSZ2 G152.47+42.11	4.81	09 29 52.64	+61 39 40.00	0.24	0.900 ; –	6	–	–	–	3	
746	PSZ2 G153.68+36.96	5.07	–	–	–	–	–	–	–	–	ND	
747	PSZ2 G153.80+33.79	4.52	–	–	–	–	–	–	–	–	ND	
754	PSZ2 G156.24+22.32	4.79	06 45 02.14	+59 27 13.30	0.75	–	–	0.30±0.05	–	–	2	
769	PSZ2 G160.94+44.85	4.98	–	–	–	–	–	–	–	–	ND	
780	PSZ2 G163.89+11.55	4.78	–	–	–	–	–	–	–	–	ND	
788	PSZ2 G165.39+09.22	5.60	05 48 09.37	+46 04 41.41	4.39	–	–	0.70±0.10	15.1±3.9	5.4	2	Clearly sub-structured, second centre at 05:48:10.56 +46:07:18.38
789	PSZ2 G165.41+25.93	4.51	07 23 27.93	+52 07 32.70	4.83	–	–	0.67±0.04	4.3±2.1	1.8	2	
797	PSZ2 G166.56–17.69	4.76	04 04 53.39	+28 18 31.85	3.44	–	–	0.70±0.07	3.3±1.8	1.4	ND	
799	PSZ2 G167.43–53.67	4.65	–	–	–	–	–	–	–	–	ND	
812 ^{a,c}	PSZ2 G171.48+16.17	4.75	06 38 00.94	+43 50 57.20	0.75	0.385 ; 0.3881	25	0.40±0.05	15.9±4.0	2.7	1	WHL J063743.6+434859
820	PSZ2 G173.76+22.92	5.80	07 17 26.66	+44 05 00.28	1.63	0.063 ; 0.0652	2	0.06±0.02	–	–	2	(5)
831 ^a	PSZ2 G177.03+32.64	4.93	08 13 08.56	+43 13 53.07	3.56	0.511 ; –	9	–	–	–	1	(1)
835	PSZ2 G179.33–22.22	5.02	–	–	–	–	–	–	–	–	ND	
836 ^{a,b}	PSZ2 G179.45–43.92	4.54	03 19 18.34	+02 05 35.60	2.58	0.397 ; 0.4005	23	0.34±0.03	19.1±4.4	5.8	1	WHL J031918.3+020535
849	PSZ2 G183.32–31.51	4.56	04 05 20.11	+07 51 26.07	2.31	–	–	0.55±0.10	1.8±1.3	0.9	3	

Table 3. Continue.

ID ¹	Planck Name	SZ SNR	Position (J2000)		Dist.(')	< z_{spec} > ; $z_{\text{spec,BCG}}$	N_{spec}	z_{phot}	R_{cor}	σ_{R}	Flag	Notes ²
			R. A.	Decl.								
852	PSZ2 G183.92+16.36	4.97	07 01 30.22	+32 54 51.20	6.61	0.091 ; 0.0914	18	0.15±0.03	30.3±5.5	4.4	1	ABELL 567
859	PSZ2 G185.68+09.82	5.18	06 37 14.93	+28 38 02.80	1.47	0.390 ; 0.3897	39	0.40±0.05	—	—	1	
860	PSZ2 G185.72−32.23	5.12	—	—	—	—	—	—	—	—	ND	
878	PSZ2 G191.57+58.88	5.17	—	—	—	—	—	—	—	—	ND	
887	PSZ2 G193.90+09.41	5.06	06 51 11.80	+21 08 10.16	0.73	0.194 ; 0.1936	29	0.16±0.03	23.5±4.8	3.0	1	
912	PSZ2 G201.20−42.83	4.70	—	—	—	—	—	—	—	—	ND	
916 ^{a,c,d}	PSZ2 G202.61−26.26	4.87	04 59 50.17	−03 16 47.52	5.52	—	—	0.23±0.03	8.5±2.9	4.6	3	WHL J045950.2−031647
917 ^{a,c}	PSZ2 G202.66+66.98	4.63	11 07 30.90	+28 51 01.20	4.68	0.482 ; 0.4814	20	0.48±0.04	11.9±3.4	5.3	1	WHL J110730+285101
920 ^{a,c,d}	PSZ2 G203.32+08.91	5.15	07 05 56.53	+12 30 33.66	4.25	—	—	0.27±0.03	9.1±3.0	4.6	2	WHL J070556.5+123034
921 ^a	PSZ2 G203.71+50.82	4.65	09 55 15.56	+26 19 37.70	2.03	0.082 ; —	22	—	—	—	1	(1)
952	PSZ2 G210.71+63.08	7.37	—	—	—	—	—	—	—	—	ND	
953	PSZ2 G210.78−36.25	6.32	—	—	—	—	—	—	—	—	ND	
982	PSZ2 G218.58+08.71	4.63	07 32 40.27	−01 03 21.55	3.40	—	—	0.55±0.05	30.7±5.5	7.6	2	1RXS J073246.4−010205
1018	PSZ2 G226.15+09.02	4.66	07 47 58.81	−07 29 22.70	2.96	—	—	0.30±0.05	28.9±5.4	10.2	2	
1023	PSZ2 G227.30+09.00	4.62	07 50 15.74	−08 24 32.56	1.85	—	—	0.24±0.03	—	—	2	1RXS J075020.3−082605
1049 ^{a,b}	PSZ2 G231.41+77.48	4.54	12 00 26.54	+22 34 19.55	6.32	0.346 ; 0.3469	2	0.35±0.03	—	—	2	WHL J120026.5+223420
1054	PSZ2 G232.27+12.59	4.52	08 12 39.17	−10 52 02.90	2.35	—	—	0.28±0.04	35.3±5.9	10.3	2	
1062	PSZ2 G233.46+25.46	4.79	—	—	—	—	—	—	—	—	ND	
1074 ^{a,b}	PSZ2 G237.68+57.83	5.36	10 53 17.80	+10 52 37.13	4.88	—	—	0.70±0.05	—	—	2	(3)
1095	PSZ2 G241.98+19.56	4.51	08 58 04.54	−14 43 01.87	3.95	—	—	0.27±0.04	33.1±5.7	8.3	2	
1151	PSZ2 G252.45+73.44	5.57	—	—	—	—	—	—	—	—	ND	
1162	PSZ2 G253.95+39.12	4.66	—	—	—	—	—	—	—	—	ND	
1168	PSZ2 G254.52+62.52	4.85	—	—	—	—	—	—	—	—	ND	
1219	PSZ2 G263.96+40.64	4.58	—	—	—	—	—	—	—	—	ND	
1262 ^{a,b}	PSZ2 G271.53+36.41	5.19	11 05 19.71	−19 59 15.61	4.73	—	—	0.50±0.03	—	—	2	WHL J110519.6−195852
1493	PSZ2 G316.43+54.02	5.18	13 23 14.77	−07 58 49.20	2.02	0.527 ; 0.5325	27	0.55±0.05	12.7±3.6	3.3	1	Sub-structured
1510 ^{a,c}	PSZ2 G320.94+83.69	7.32	13 00 05.74	+21 01 28.29	7.00	0.461 ; 0.4612	5	0.45±0.04	—	—	3	
1513	PSZ2 G321.94+75.57	4.66	—	—	—	—	—	—	—	—	ND	
1532	PSZ2 G325.19+49.12	4.62	13 49 55.18	−11 15 24.44	3.61	—	—	0.20±0.03	28.1±5.3	6.5	2	WHY J135000.5−111724
1548 ^{a,b}	PSZ2 G328.96+71.97	5.85	13 23 02.10	+11 01 32.12	18.03	0.090 ; 0.0937	94	0.09±0.01	—	—	3	

¹ SZ targets identified with the ID followed by an A or B label indicate the presence of multiple counterparts.² References. (1) Burenin (2017), (2) Rykoff et al. (2014), (3) Burenin et al. (2018), (4) Zaznubin et al. (2019), (5) Boada et al. (2019)^a Photometric and/or spectroscopic redshift obtained from SDSS DR14 data.^b Already confirmed in Streblyanska et al. (2018)^c Classified as "potentially associated" in Streblyanska et al. (2018)^d Richness study from PAN-STARRS

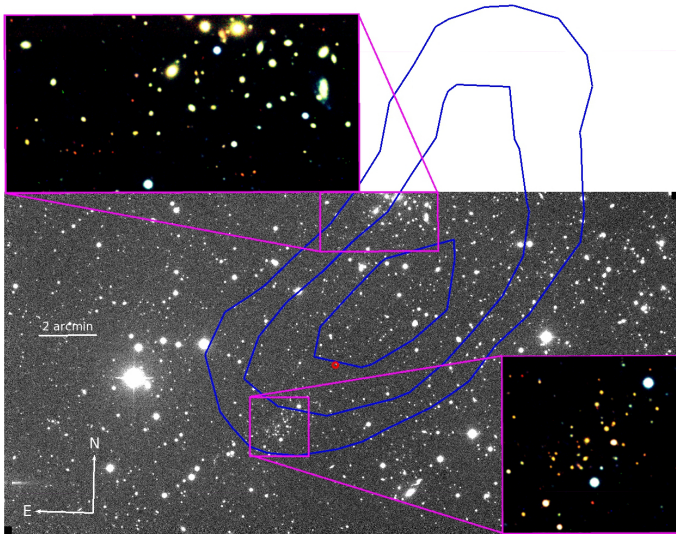


Fig. 6. Compton y-map superimposed on the INT r' -band of the PSZ2 G130.64+37.16. Blue contours correspond to the $4, 4.6$ and 5.2×10^{-6} levels of the Compton y-map in this area. The nominal SZ pointing (red) is clearly closer to the cluster named 644-A (zoomed in the lower-right region) which presents 14 spectroscopic members and shows a velocity dispersion close to 1000 km s^{-1} ; the cluster named 644-B (zoomed in the upper-left region) is $6'.07$ away from the SZ centre but the MILCA y-map shows that the contours are elongated along this counterpart location which is twice as rich as the 644-A.

4.1. Notes on individual objects

PSZ2 G058.31+41.96 This candidate is flagged as a non-detection due to a bright star located near the *Planck* pointing. The star prevents photometric measurements of this region, and thus, we are unable to visually identify an over-density of galaxies. Despite this problem, we cannot identify visually any over-density of galaxies in the region.

PSZ2 G104.52+39.39 The distance from the optical centre and the *Planck* nominal pointing is $5'.62$. Nevertheless, we validate this cluster with Flag 2 because the MILCA y-map contours are elongated along the line that links both optical and *Planck* centres. Besides this fact, the position error in the *Planck* catalogue is too high ($5'.40$) compared to the nominal one ($2'.43$).

PSZ2 G130.64+37.16 This candidate has two optical counterparts validated already in Streblyanska et al. (2018) and one of them in Burenin (2017). This is a tricky case as it is shown in Fig. 6. The nominal SZ pointing is clearly closer to the cluster named 644-A which presents 14 spectroscopic members and shows a velocity dispersion close to 1000 km s^{-1} ; the cluster named 644-B is $6'.07$ away from the SZ centre but the MILCA y-map shows that the contours are elongated along this counterpart location which is twice as rich as the 644-A. This is also a case where the position error in the *Planck* catalogue is $5'.38$ which is more than twice the mean position error.

PSZ2 G146.13+40.97 The optical centre of the proposed counterpart (its BCG) is at $7'.18$ away from the *Planck* SZ pointing, which is affected by a position error of $5'.89$. The y-map contours present a very irregular shape, maybe due to galactic dust contamination around this region. We estimate a richness of $\sigma_R = 3.5$ for this system and we find four cluster members at $z_{\text{spec}} = 0.342$ in the SDSS DR14 spectroscopic sample. So, we classify this counterpart with Flag= 2. The ultimate confirmation will be obtained using MOS observations.

PSZ2 G152.47+42.11 We find a possible cluster counterpart at $z_{\text{spec}} = 0.900$. The deepness of our images makes it impossible to estimate the richness at this redshift. However, we have observed this system spectroscopically and we have found six cluster members. From these six galaxies, we obtain a very low-velocity dispersion ($< 400 \text{ km s}^{-1}$), revealing a low-mass galaxy system. Thus, in this case, we classify this optical counterpart with Flag= 3.

PSZ2 G156.24+22.32 This region encloses two very bright stars, making it very difficult to obtain accurate photometry or richness. However, by eye inspection, we identify a cluster showing a galaxy population with coherent colours. A detailed study of the photometry of some individual likely members and the BCG reveals a $z_{\text{phot}} = 0.30$. In addition, the y-map contours present a very regular profile centred on this system. For all these reasons, we classify this system with Flag= 2.

PSZ2 G177.03+32.64 Burenin (2017) reports a counterpart for this candidate at $z \sim 0.28$. We have analysed this over-density finding seven galaxies with spectroscopic redshifts in the SDSS archive. Four of these galaxies are more than 4 Mpc away from the *Planck* centre and the velocity dispersion accounting for the seven galaxies is less than 300 km s^{-1} . For this reason, we present here only one counterpart at $z_{\text{spec}} = 0.511$ whose velocity dispersion, calculated using 9 members is approximately 1000 km s^{-1} .

PSZ2 G183.92+16.36 The distance between the BCG of this cluster and the *Planck* pointing is $6'.61$, which is only 0.67 Mpc at the redshift of the cluster, $z_{\text{spec}} = 0.091$ (see Fig 4). We perform multi-object spectroscopy and retrieve 18 cluster members, showing a $\sigma_v \sim 650 \text{ km s}^{-1}$. In addition, this cluster is known as Abell 567, which is well consolidated by other observations in the past (Abell et al. 1989). Therefore, we confirm Abell 567 as the counterpart of this SZ source, classifying it as Flag= 1.

PSZ2 G202.61+26.26 and PSZ2 G203.32+08.91 Both candidates were analysed using PANSTARRS photometric data (Chambers et al. 2016). Both systems are rich but the optical centre of the first one is more than $5'$ away from the *Planck* nominal pointing, so classified as Flag 3.

PSZ2 G227.30+09.00 This is an SZ source placed at very low galactic latitude, so a large number of stars are crowding this field. For this reason, we were not able to compute the richness: the galaxies of the background are partially masked by the foreground stars. However, this system presents X-ray emission and has been catalogued as 1RXS J075020.3-082605 in the ROSAT survey. So, we classify this source as Flag= 2.

PSZ2 G237.68+57.83 This cluster has been already validated by Streblyanska et al. (2018) using SDSS data. Here, we confirm this association using the INT images. Despite we are not able to perform a richness estimation at this redshift, some individual likely cluster members show photometry in agreement with a $z_{\text{phot}} = 0.70 \pm 0.05$. We also find two additional over-densities at (RA=10:53:35.55, Dec=+10:43:45.71) and (RA=10:53:59.602, Dec=+10:46:38.23). However they are at over $> 10'$ distance from the SZ coordinates and thus, probably not contributing to the SZ signal. Therefore we validate PSZ2 G237.68+57.83 as a single counterpart at $z_{\text{phot}} = 0.70$.

PSZ2 G271.53+36.41 This candidate was confirmed photometrically in Streblyanska et al. (2018) as a double detection. However, only one cluster is visible in the INT images. This cluster is at $z_{\text{phot}} = 0.50 \pm 0.03$. No more systems are associated with this SZ source.

PSZ2 G328.96+71.97 was validated by Streblyanska et al. (2018) using SDSS DR12 data. Here, we use new spectroscopic information provided by SDSS DR14 in order to update

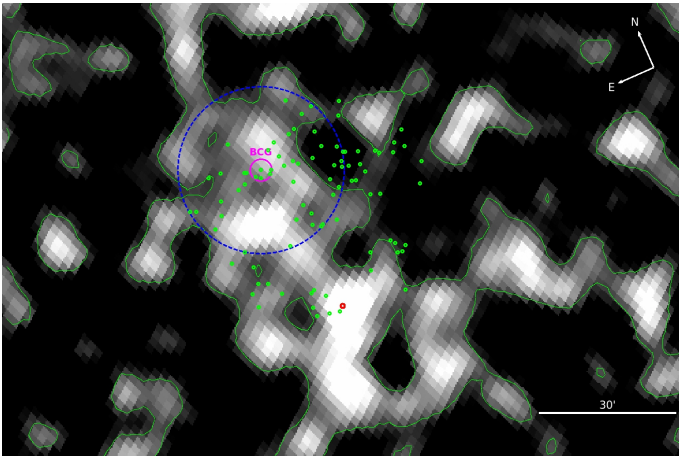


Fig. 7. SZ emission as seen in the Compton y -maps for the source PSZ2 G328.96+71.97. The red dot represents the SZ coordinate as it appears in the PSZ2 catalogue. The BCG of the cluster is plotted in magenta, while the rest of the galaxies members are shown in green. The blue circle encloses the virial radius of this cluster. The 94 cluster members are placed completely off the SZ peak and the optical counterpart of this SZ source remains unknown.

the information there reported. We find 94 cluster members at $< z_{\text{spec}} >= 0.090$. However, the BCG of this structure is at $34.6'$ from the *Planck* pointing. Fig. 7 shows the scenario around this region. SZ emission presents a very spread and irregular profile, with several peaks. The 94 cluster members present a $\sigma_v \sim 800 \text{ km s}^{-1}$ and a virial radius of 1.6 Mpc , but the cluster seems to be placed completely off the SZ peak. Notice that the distance between the *Planck* pointing and the optical cluster centre is larger (double) than the virial radius of the cluster. So, for all these reasons, we conclude that no optical counterpart is found for this SZ source, and the actual counterpart (if it exists) is still unknown.

5. Observations of other PSZ2 candidates beyond the LP15 sample

In the PSZ2 catalogue, there are 73 clusters validated using the AllWISE mid-infrared source catalogue (Cutri et al. 2013). This catalogue is based on the observations from the Wide-field Infrared Survey Explorer mission (WISE, Wright et al. 2010). Using the (W1-W2) colour they search for galaxy over-densities in the redshift range $0.3 < z < 1.5$. The details of this validation process can be found in Sect. 7.4 in Planck Collaboration XXVII (2016). Those objects had `validation` = 16 in the original PSZ2 catalogue, and thus, they were not included in the definition of the LP15 sample.

Here, we present an update on 38 of those ALLWISE sources, providing their spectroscopic redshifts which were obtained using dedicated observations carried out with the telescope time within the LP15 programme. Table 5 presents this information, and it is organised in the same way as Table 3.

The double detections PSZ2 G086.28+74.76, PSZ2 G139.00+50.92 and PSZ2 G141.98+69.31 can be considered single detection even if secondary clusters are detected, because they are very low mass systems, and so not capable of contributing significantly to the SZ signal.

As noted in earlier by the Planck Collaboration, the number of double cluster detections is relatively high, as compared to

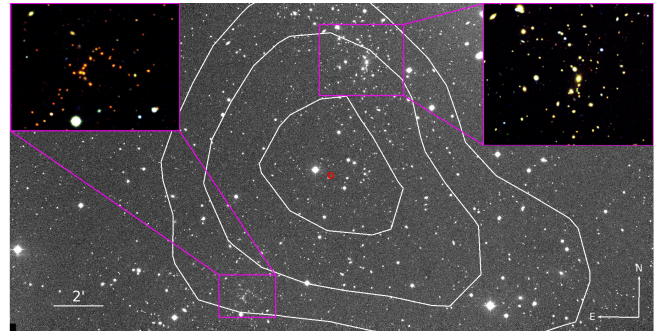


Fig. 8. Compton y -map superimposed to the INT r' -band of the PSZ2 G076.55+60.29. White contours correspond to the $3, 4$ and 5×10^{-6} levels of the Compton y -map in this area. The *Planck* nominal pointing is represented in red. In the upper corners we show zoomed RGB images of the 327-A (left) and 327-B (right), respectively. Both systems, at $z_{\text{spec}} = 0.632$ and $z_{\text{spec}} = 0.287$, are associated with this SZ signal. This is a clear example of a multiple detection.

other surveys, either in X-rays (Planck Collaboration int. I 2012) or in optical (Planck Collaboration int. XXVI 2015).

We have cross-checked our sample with two galaxy cluster catalogues WHL (Wen et al. 2012) and WHY (Wen & Han 2018), based on optical and infrared data, respectively. WHL catalogue was published using SDSS data, while WHY used 2MASS (Skrutskie et al. 2006), WISE Wright et al. (2010) and SuperCOSMOS (Hambly et al. 2001) data. We only find three matches with WHL. PSZ2 G076.55+60.29 and PSZ2 G141.98+69.31 will be discussed in the next sub-section, and PSZ2 G021.02–29.0 which is also part of the WHY catalogue. We find seven matches with the WHY catalogue, we are in a 1σ agreement in redshift except for PSZ2 G056.38+23.36. In this case, we estimate a photometric redshift of $z_{\text{phot}} = 0.21 \pm 0.02$ while Wen & Han (2018) reports $z_{\text{phot}} = 0.31 \pm 0.04$, compatible within 2σ .

We also present in this section an update on four sources that were already confirmed in the PSZ2 original catalogue Planck Collaboration XXVII (2016) as they were matched with PSZ1 clusters but without an estimation of their redshifts. Here, we provide the photometric redshift for three of them and invalidate the already confirmed PSZ2 G198.73+13.34, for which we are unable to find any galaxy over-density. In a future publication, we will discuss this type of sources that we believe are false validations. These four sources can be found in table 4.

5.1. Discussion on special cases

We found that PSZ2 G076.55+60.29, which it was classified as an individual counterpart by Streblyanska et al. (2018), is, in fact, a superposition of two clusters, at $z_{\text{spec}} = 0.287$ and $z_{\text{spec}} = 0.632$, respectively. The first one (327-A) was already proposed as potentially associated cluster. Here, we confirmed it with 5 spectroscopic members. The distance to the *Planck* nominal pointing of the second counterpart (327-B) is slightly greater than $5'$ but the MILCA y -map contours superimposed on an INT image (Fig. 8) show that the SZ emission is clearly a superposition of both clusters. Both counterparts are two of the richest systems studied in this work, presenting a σ_R of 23.1 and 8.4, respectively.

PSZ2 G086.28+74.76 We find two clusters around the SZ emission at $z_{\text{spec}} = 0.246$ and $z_{\text{spec}} = 0.701$ which we name 381-A and 381-B, respectively. Both present high-velocity dispersion. However, the centre of 381-A is $8.93'$ away from the

Table 4. Update of already known optical counterparts from the PSZ1.

ID	Planck Name	SZ SNR	R. A.	Decl.	Dist.(')	z_{phot}	R_{cor}	σ_R	Flag	PSZ1 Name
897	PSZ2 G196.65–45.51	4.91	03 42 54.40	–08 41 07.70	1.52	0.25±0.03	–	–	2	PSZ1 G196.62–45.50
901	PSZ2 G198.73+13.34	6.03	–	–	–	–	–	–	ND	PSZ1 G198.67+13.34
1130	PSZ2 G249.14+28.98	5.96	09 44 57.60	–13 48 11.22	1.16	0.15±0.03	18.6±4.3	5.3	2	PSZ1 G249.14+28.98
1539	PSZ2 G326.73+54.80	5.92	13 45 14.70	–05 32 04.00	3.91	0.46±0.05	20.3±4.5	10.6	2	PSZ1 G326.64+54.79

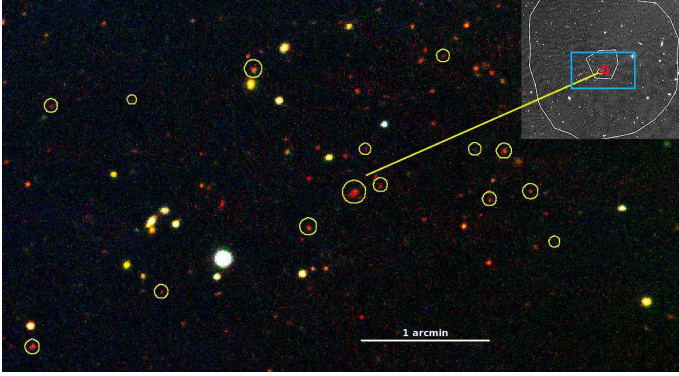


Fig. 9. The zoomed RGB image of the central area of high- z cluster ($z_{\text{spec}} = 0.816$) associated with PSZ2 G126.57+51.61. We marked as a yellow circles cluster members confirmed spectroscopically. The small top panel shows the WFC/INT i' -band image with white contours corresponding to the 3 and 6×10^{-6} levels of the Compton y -map in this area. The red circle indicates the nominal PSZ2 position. The blue square shows the size of the area presented in the main RGB image.

Planck centre. So we conclude that this source has only one optical counterpart at $z_{\text{spec}} = 0.701$.

PSZ2 G126.57+51.61 is one of the most distant cluster in our sample, at $z_{\text{spec}} = 0.816$. Burenin et al. (2018) published confirmation of one galaxy at $z_{\text{spec}} = 0.815$. This cluster is at the detection limits of our deep optical images, with most of the members detected almost at the noise level of the i' -band image. No RS for this cluster could be constructed. However, inspection of the RGB image revealed an over-density of red sources close to the *Planck* position supported by the contours extracted from the MILCA y -map (Fig. 9). Our spectroscopic data together with SDSS data confirm this cluster with 20 members and a $\sigma_v \sim 850 \text{ km s}^{-1}$.

PSZ2 G133.92–42.73 There is a potential counterpart but it is discarded due to its low σ_R . Looking at the RGB image (left panel, Fig. 10) it seems to be a high redshift cluster as seen in the WISE image (right panel, Fig. 10). In SDSS there are three galaxies with $z_{\text{spec}} \sim 0.581$ but they are not associated with any galaxy over-density. Deeper imaging or spectroscopic observations would be needed in order to reject the possibility of a high- z ($z > 0.8$) cluster.

PSZ2 G139.00+50.92 was already confirmed by Streblyanska et al. (2018) at $z_{\text{phot}} = 0.6$. We have performed spectroscopic observations for this cluster, named 681-A in this work, finding a velocity dispersion below the confirmation limit ($\sigma_v < 650 \text{ km s}^{-1}$). We conclude that it is not the main counterpart to the SZ emission. However, we find another cluster (681-B) at $z_{\text{spec}} = 0.784$ showing a $\sigma_v > 800 \text{ km s}^{-1}$, so we conclude that this last counterpart is the responsible for the SZ emission.

PSZ2 G141.98+69.31 This is a case of double detection. We find two over-densities in this field but once we made spectroscopic observations and calculate the velocity dispersion, we re-

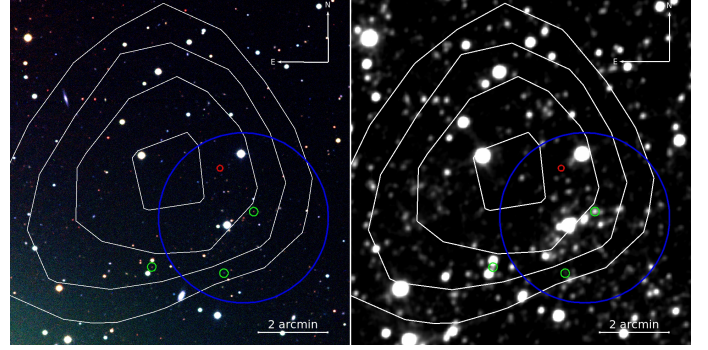


Fig. 10. Left: RGB image of the source PSZ2 G133.92–42.73. Right: WISE W1-band of the same region. In both images Compton y -maps are represented in white ($5, 5.8, 6.6$ and 7.4×10^{-6} levels). The blue region corresponds to 1 Mpc (2.45) at the mean redshift of the three galaxies represented in green. The *Planck* nominal pointing is marked in red.

alised that the object named 690-B presented a $\sigma_v < 400 \text{ km s}^{-1}$, very low to be associated with the SZ emission. Consequently, we only validate the object proposed in Streblyanska et al. (2018) with a spectroscopic redshift of $z_{\text{spec}} = 0.713$, here named as 690-A.

PSZ2 G270.78+36.83 This candidate was already validated by Streblyanska et al. (2018) as a double detection. Here, we spectroscopically confirm one of these counterparts by detecting 25 cluster members at $z_{\text{spec}} = 0.516$, showing a $\sigma_v \sim 900 \text{ km s}^{-1}$. The second counterpart remains unconfirmed spectroscopically.

Table 5. Updated information of other PSZ2 candidates beyond the LP15 sample.

ID ¹	Planck Name	SZ SNR	Position (J2000)		Dist.(')	< z _{spec} > ; z _{spec} ,BCG	N _{spec}	z _{phot}	R _{cor}	σ_R	Flag	Notes ²
			R. A.	Decl.								
65	PSZ2 G020.21–36.84	5.17	20 51 57.42	–25 29 17.03	1.07	–	–	0.21±0.02	18.1±4.3	3.6	2	
68 ^{a,c}	PSZ2 G021.02–29.04	4.89	20 20 28.21	–22 25 14.78	1.83	0.300 ; 0.3017	25	0.32±0.04	–	–	1	WHY/WHL J202028.2–222515
92	PSZ2 G027.77–49.72	4.60	21 53 03.42	–23 34 13.08	1.45	0.165 ; 0.1641	15	0.12±0.02	20.6±4.5	4.4	1	2dF Survey, (1)
93	PSZ2 G027.81–45.93	5.24	21 37 16.11	–22 32 19.80	2.23	–	–	0.45±0.05	15.8±4.0	5.2	2	
120	PSZ2 G033.83–46.57	5.53	21 45 12.35	–18 42 57.41	2.50	–	–	0.32±0.04	3.7±1.9	1.7	2	WHY J214532.4–184130, (2)
206	PSZ2 G050.98–61.48	5.10	22 58 53.05	–15 35 30.87	1.76	–	–	0.18±0.03	14.2±3.8	6.5	2	
227	PSZ2 G056.38+23.36	4.85	18 01 16.53	+30 23 20.71	3.43	–	–	0.21±0.02	11.4±3.4	7.0	2	WHY J180116.5+302321
277 ^{a,c}	PSZ2 G066.34+26.14	5.63	18 01 06.52	+39 52 06.73	1.64	0.622 ; 0.6167	52	0.63±0.06	–	–	1	
282	PSZ2 G066.85+22.48	4.88	18 20 08.12	+39 15 52.93	2.05	–	–	0.19±0.02	22.3±4.7	10.3	2	WHY J182008.2+391553
294 ^{a,c}	PSZ2 G069.39+68.05	4.51	14 21 38.32	+38 21 17.54	0.46	0.766 ; 0.7630	23	0.70±0.06	–	–	1	CIG-J142138.3+382118, (3)
304 ^b	PSZ2 G071.82–56.55	4.78	23 09 37.35	–04 09 52.17	1.20	0.822 ; –	38	–	–	–	1	
323	PSZ2 G075.85+15.53	4.64	19 10 50.62	+44 54 48.99	3.30	–	–	0.30±0.03	7.8±2.8	7.3	2	
327-A ^{a,d}	PSZ2 G076.55+60.29	5.42	14 52 00.51	+44 31 21.31	4.21	0.287 ; –	5	0.25±0.03	35.9±6.0	23.1	2	WHL J145206.4+443235
327-B ^a			14 52 24.24	+44 22 56.58	5.33	0.632 ; –	1	0.70±0.06	14.5±3.8	8.4	2	
333	PSZ2 G078.10–83.83	4.87	00 32 30.94	–22 42 10.95	2.00	–	–	0.28±0.03	18.4±4.3	8.7	2	
355	PSZ2 G082.37+22.35	5.93	18 44 31.37	+53 00 09.01	0.60	–	–	0.29±0.03	14.5±3.8	9.3	2	
359	PSZ2 G083.56+24.90	6.13	18 29 28.55	+54 43 08.80	1.67	–	–	0.32±0.04	7.0±2.6	2.7	2	
378	PSZ2 G085.95+25.23	5.55	18 30 23.81	+56 53 11.12	0.62	–	–	0.65±0.05	4.6±2.1	1.5	2	
381-A	PSZ2 G086.28+74.76	5.07	13 38 40.43	+38 52 32.57	8.93	0.246 ; –	20	–	–	–	3	
381-B ^{a,c}			13 37 54.11	+38 53 30.94	1.28	0.701 ; –	21	0.80±0.06	–	–	1	
394 ^{a,c}	PSZ2 G087.39–34.58	4.62	22 49 09.53	+19 44 30.50	1.93	0.772 ; –	31	0.70±0.07	–	–	1	(4)
468	PSZ2 G098.75–28.63	4.74	–	–	–	–	–	–	–	–	ND	
475	PSZ2 G099.55+34.23	5.34	17 10 33.34	+68 44 43.60	1.01	–	–	0.31±0.03	15.4±3.9	6.0	2	WHY J171033.4+684443
548	PSZ2 G113.27+48.39	5.30	13 58 59.49	+67 25 50.29	0.75	–	–	0.32±0.03	7.9±2.8	4.5	2	
581	PSZ2 G118.49+48.17	5.16	13 23 55.03	+68 39 30.73	1.09	–	–	0.35±0.03	24.4±4.9	6.2	2	WHY J132355.0+683931
582	PSZ2 G118.56–13.14	4.63	00 25 13.35	+49 30 35.84	0.50	–	–	0.23±0.03	20.9±4.6	3.7	2	
590	PSZ2 G120.30+44.47	5.31	13 16 38.50	+72 32 15.60	1.09	–	–	0.23±0.03	23.3±4.8	7.9	2	WHY J131638.6+723217
623 ^b	PSZ2 G126.28+65.62	4.67	12 42 23.33	+51 26 20.98	1.67	0.819 ; 0.8201	16	–	–	–	1	(4)
625 ^{a,c}	PSZ2 G126.57+51.61	6.35	12 29 47.56	+65 21 13.41	0.33	0.817 ; –	20	0.80±0.10	–	–	1	(4)
654 ^a	PSZ2 G133.92–42.73	4.70	01 25 33.36	+19 22 53.51	1.65	0.581 ; –	3	0.65±0.07	2.3±1.5	1.1	ND	
681-A	PSZ2 G139.00+50.92	4.98	11 20 22.76	+63 14 38.35	1.63	0.636 ; –	13	–	–	–	3	
681-B			11 20 27.45	+63 14 46.15	2.04	0.784 ; –	11	–	–	–	1	
690-A ^{a,d}	PSZ2 G141.98+69.31	4.71	12 12 38.98	+46 21 06.46	3.25	0.713 ; –	16	0.70±0.06	–	–	1	WHL J121240.6+462123
690-B			12 12 42.63	+46 21 04.59	2.65	0.796 ; –	9	–	–	–	3	
701	PSZ2 G144.23–18.19	5.22	02 38 55.30	+40 11 11.57	0.41	–	–	0.31±0.03	13.4±3.7	2.2	2	
764	PSZ2 G159.40–40.67	5.05	02 42 22.99	+14 15 14.60	2.81	–	–	0.22±0.03	23.2±4.8	5.4	2	
768	PSZ2 G160.83–70.63	6.30	01 39 20.72	–11 22 19.49	1.20	–	–	0.24±0.03	26.2±5.1	7.7	2	
810 ^{a,c}	PSZ2 G171.08–80.38	4.90	01 21 53.44	–20 33 26.45	2.67	0.313 ; 0.3134	33	0.33±0.03	–	–	1	WHL J012153.4–203327
902 ^b	PSZ2 G198.80–57.57	4.83	03 02 06.58	–15 33 41.69	0.53	0.530 ; 0.5292	16	–	–	–	1	
937 ^b	PSZ2 G208.57–44.31	4.53	04 02 36.08	–15 40 49.56	1.47	0.820 ; 0.8196	17	–	–	–	1	
1254 ^{a,c}	PSZ2 G270.78+36.83	4.99	11 04 21.06	–19 14 18.34	2.55	0.516 ; 0.5146	25	0.52±0.05	–	–	1	Double detection in (5)
1606	PSZ2 G343.46+52.65	4.89	14 24 23.15	–02 43 49.34	0.88	0.711 ; –	20	0.70±0.07	–	–	1	(4)

¹ SZ targets identified with the ID followed by an A or B label indicate the presence of multiple counterparts.² References. (1) De Propriis et al. (2002), (2) Amodio et al. (2018), (3) Buddendiek et al. (2015), (4) Burenin et al. (2018), (5) Streblyanska et al. (2018)^a Photometric and/or spectroscopic redshift obtained from SDSS DR14 data.^b No imaging performed, private communication with Saclay group^c Already confirmed in Streblyanska et al. (2018)^d Classified as "potentially associated" in Streblyanska et al. (2018)

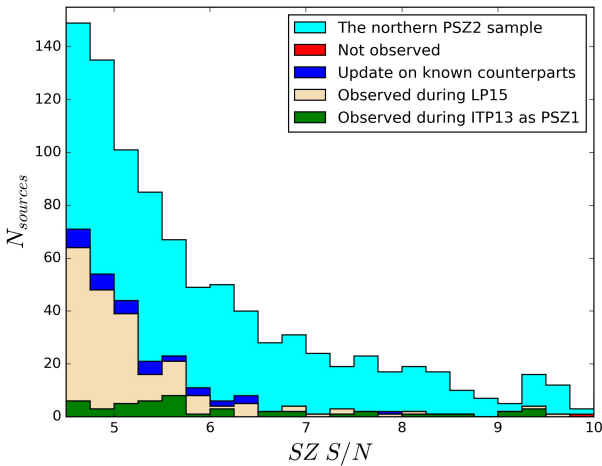


Fig. 11. PSZ2 cluster counts as a function of the signal-to-noise ratio of the SZ detection S/N . The PSZ2-North sample is represented in light blue, the sources still not observed are represented in red ($< 0.5\%$), the updated sources described in Sect. 5 are shown in dark blue (3.4%) and the sources originally not confirmed that were observed during LP15 and ITP13 are shown in green (18.4% and 4.8% , respectively). The bin size is 0.25.

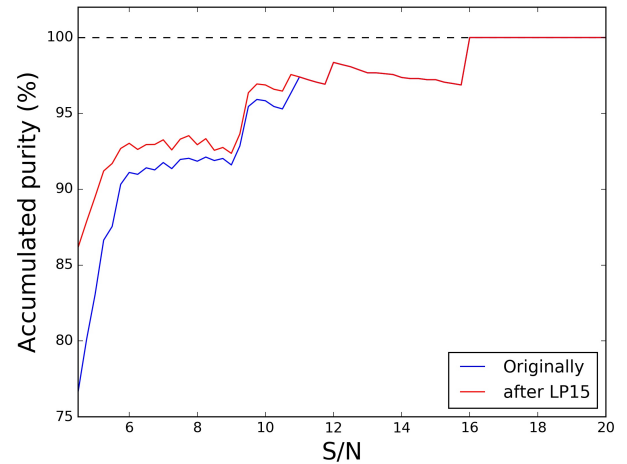


Fig. 12. Accumulated purity of the PSZ2-North sample ($Dec. > -15^\circ$) studied as a function of the S/N , i.e. the percentage of the sources that are actual clusters and related to the SZ signal. In blue we represent the original purity of the catalogue and in red the same purity but after this work.

6. On PSZ2 statistics in the northern sky

In PSZ2 catalogue there are 1003 sources with $Dec. > -15^\circ$. After the two years of LP15 observations, a total of 226 sources have been observed; 184 of them were part of the LP15 sample and thus were not validated at the time the PSZ2 catalogue was published. In addition, we updated the redshift for 42 additional sources. In this section, we will carry out the statistical analysis of this “northern sky” sub-sample of the PSZ2, such as the purity and effects that can influence the PSZ detection. For definiteness, we will refer to this sub-sample as PSZ2-North, which represents the 60 % of the complete PSZ2 sample.

We note that this PSZ2-North sample also includes some PSZ2 sources associated with PSZ1 objects, that were observed during the ITP13 (Planck Collaboration int. XXXVI 2016; Barrena et al. 2018). There are still five sources ($< 0.5\%$) that could not be observed in order to validate the full PSZ2-North, so we exclude them of the sample for the computation of the statistics in this section.

Figure 11 shows the number of clusters as a function of the signal-to-noise ratio in the catalogue. The vast majority of the sources studied in this work present $S/N < 6$ and it is within this range where this optical follow-up has performed the largest contribution. In particular, we observed 37% of the sources with $4.5 < S/N < 6$.

We define the purity as the ratio between confirmed clusters and the total number of SZ sources. It is important to take into account that we have explored the optical range in which the dust emission could be masking the possible counterpart, later in this section we quantify this effect. Figure 12 shows the accumulated purity of the PSZ2-North sample as a function of the S/N . While originally, it showed a purity of 76.7 %, after every validation programme to date, the purity increases up to 86.2 % for $S/N > 4.5$. The feature in Fig. 12 showing a decrease of purity in the range $12 < S/N < 16$ is due to the existence of one non-detection listed in the PSZ2 as high S/N source (PSZ2 G153.56+36.82), studied in detail in Paper I.

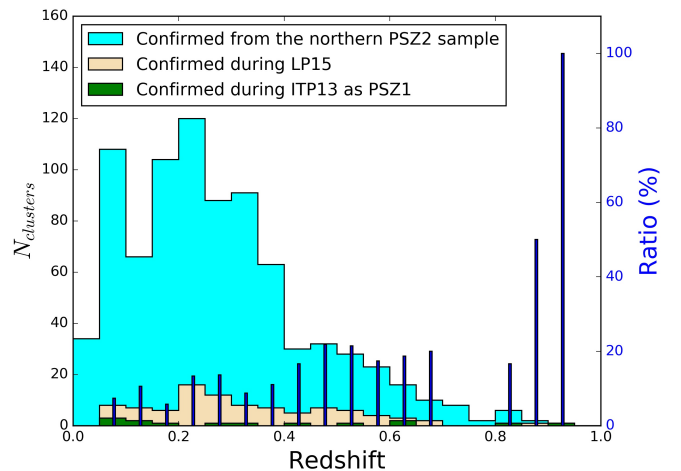


Fig. 13. Cluster counts as a function of redshift. Colour codes are the same as in Fig. 11. Dark blue bars represent the ratio between clusters confirmed during our follow-ups and the total confirmed clusters. The size of the redshift bin is 0.05.

Figure 13 shows the distribution of redshifts of the *Planck* confirmed clusters. We note that 77 % of them present a redshift between $0.05 < z < 0.4$ which is the optimal range for the cluster detection of the *Planck* mission. The median redshift of the PSZ2-North sample is 0.23 while the median redshift of the clusters confirmed during LP15 is 0.29. While we confirm about 10 % of the clusters at $z < 0.4$, this rate is $\sim 20\%$ for $z > 0.4$. Moreover, we confirmed in Barrena et al. (2018) the most distant *Planck* SZ cluster in the northern hemisphere: the PSZ2 G123.35+25.39, at $z_{\text{phot}} = 0.95$.

Burenin (2017) presented an extension for the PSZ2 catalogue using SDSS and WISE. We find 28 matches between this catalogue and the LP15 sample. Our results are in good agreement for the majority of the sources. For PSZ2 G069.47–29.06 and PSZ2 G130.64+37.16, the author only reports one counterpart, while we find two. PSZ2 G069.47–29.06 was discussed in Paper I, where both candidates were confirmed presenting 44

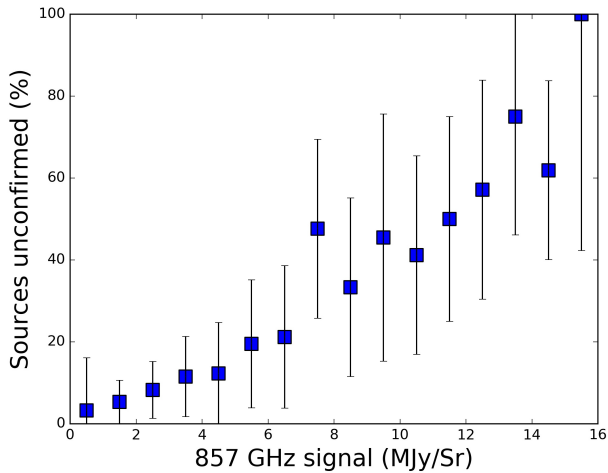


Fig. 14. Ratio between unconfirmed and total number of sources for the PSZ2-North sample (Dec. $> -15^\circ$) as a function of the 857 GHz signal in bins of 1 MJy sr^{-1} . Error bars correspond to a Poisson error in the distribution of total number of sources.

and 30 spectroscopic members, as mentioned in Zaznabin et al. (2019). PSZ2 G130.64+37.16 was discussed in Sect. 4.1. On the contrary, for PSZ2 G066.59–58.51, we find only one counterpart, while Burenin (2017) reports more than one.

We compare our results with those of (Zohren et al. 2019, in prep., private communication). They use the WHT to validate high- z clusters of the *Planck* catalogues. They report the redshift, richness and mass for 23 candidates. Twenty of them were also observed during the LP15 programme. We agree with their results but for three cases. They claim as well as Burenin et al. (2018) that PSZ2 092.69+59.92 has two counterparts, at $z = 0.46$ and $z = 0.84$. Our spectroscopic observations reveal that the galaxy over-density at $z = 0.84$ is a low mass system as it presents $\sigma_v < 450 \text{ km s}^{-1}$. They found PSZ2 G139.00+50.92 presents a mass below their limit for validation. As discussed in Sect. 5.1, we find two possible counterparts, one of them (681-B) showing a $\sigma_v > 800 \text{ km s}^{-1}$. PSZ2 G165.41+25.93 is also below their mass limit whereas in our richness analysis it shows a $\sigma_R = 1.8$, just above our validation limit of $\sigma_R = 1.5$.

We also compare our results with Zaznabin et al. (2019) where the authors report 38 spectroscopic redshift for PSZ2 candidates. We find 20 matches between this catalogue and the LP15 sample. We find discrepancies in only one case: PSZ2 G202.61–26.26. The authors report three spectroscopic redshifts at $z_{\text{spec}} = 0.533$ while we find a galaxy over-density at $z_{\text{phot}} = 0.23$ but further than $5'$ away from the *Planck* centre, so not linked to the SZ emission.

In order to study the galactic disturbance on the SZ *Planck* detection, we compute the number of non-detections as a function of the 857 GHz signal in the *Planck* map. This map could be used as a tracer of the thermal dust emission (Planck Collaboration XI 2014). The signal is computed as the mean value within a region of 0.5° radius around the nominal pointing in the PSZ2 catalogue. Figure 14 represents the ratio between unconfirmed and total number of sources for the PSZ2-North sample as a function of the 857 GHz signal in bins of 1 MJy sr^{-1} . This figure shows a clear correlation between these two magnitudes. Below 7 MJy sr^{-1} the ratio of unconfirmed sources is under 20%. However, in zones with high dust emission (mainly places in the galactic plane), the false SZ clusters can be higher than 60–70%.

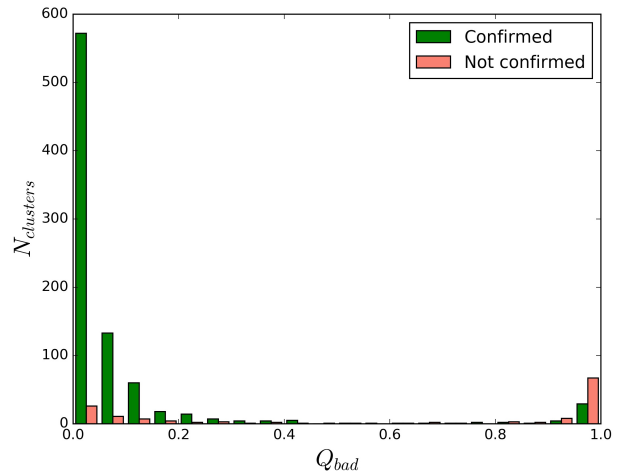


Fig. 15. Number of cluster-candidates versus the neural network quality flag value for the PSZ2-North sample. The confirmed candidates are represented in green while the still not confirmed are shown in red. The bin size is 0.05.

Figure 15 shows the number of cluster-candidates versus the neural network quality flag value for the PSZ2-North sample (Q_{bad}). This value was defined in Aghanim et al. (2015), it is an indicator of the reliability of a SZ source to be a real galaxy cluster. Candidates presenting values of $Q_{\text{bad}} > 0.6$ are considered low reliable sources. In the PSZ2-North sample, we observe that the vast majority ($> 93\%$) of the clusters with $Q_{\text{bad}} < 0.6$ are actual clusters while less than 33% with $Q_{\text{bad}} > 0.6$ are confirmed.

We also compare the full validation results with Khatri (2016) where the author published a method of validation for the PSZ2 catalogue based on the combination of CO and y -distortion maps. He classifies the sources in five different groups depending on the value of his estimator: *MOC*, *pMOC*, *CLG*, *pCLG* and *IND*. The signal of the sources classified as *MOC* and *pMOC* is considered to come from molecular clouds while *CLG* and *pCLG* come from galaxy clusters. *IND* is indeterminable. We find that 95.2% of the *IND* and 94.6% of the *CLG* + *pCLG* correspond to actual validated clusters. On the other hand, 64.7% of the *MOC* + *pMOC* are also validated clusters. We expected that the sources with this classification present a lower rate of validation, however, it is not the case. A possible explanation for these results is that the threshold used by Khatri (2016) to distinguish between molecular clouds and clusters was shifted towards high values of $\Delta(\Sigma\chi^2)_{\text{CO-}y}$. To illustrate this fact, for the 59 sources that the author classifies as *pMOC*, 48 (81.3%) are actual clusters. A full study on this matter will be approached in a future publication where we will discuss the properties of the clusters, velocity dispersion, masses and their relations with the SZ signal.

7. Conclusions

This work presents the final results of the observational programme LP15 started in Paper I. We report here about the second year of observations carried out using INT, TNG and GTC at ORM Observatory, as part of the optical follow-up confirmation and characterization programme of *Planck* SZ sources in the northern hemisphere.

During the second year of observations, 78 PSZ2 sources with no known optical counterpart have been observed. Thanks

to a robust confirmation criterion based on velocity dispersion, when available, and richness estimations we were able to confirm 40 candidates, providing 18 spectroscopic and 22 photometric redshifts.

We update the information on 42 sources that were already validated in the original PSZ2 catalogue but presented no redshift estimation. We provide spectroscopic redshift for 20 of them and photometric redshift for 20. We also perform the richness study and apply the same criteria as for the candidates in order to check the associations to the SZ signal. We discover that three already confirmed counterparts were not present in the optical range studied here.

At the end of the whole observational programme LP15, we were able to confirm 81 new cluster candidates, with a median redshift of 0.29 while the mean redshift of the catalogue is 0.23. Our main contribution appears in the redshift interval $0.4 < z < 0.7$, where our confirmations correspond to 20 % of the total clusters confirmed in the PSZ2 in that range. The purity of the catalogue has been updated from 76.7 % to 86.2 %.

Finally, we found a clear correlation between the number of unconfirmed sources and galactic thermal dust emission. This correlation suggests that there are spurious detections inside the PSZ2 catalogue. Some of these false detections have been discussed here. In particular, we find that more than 50 % of the sources with a mean signal in the 857 GHz maps greater than 7 MJy/sr remain unconfirmed after this work.

Acknowledgements. This article is based on observations made with a) the Gran Telescopio Canarias operated by the Instituto de Astrofísica de Canarias, b) the Isaac Newton Telescope, and the William Herschel Telescope operated by the Isaac Newton Group of Telescopes, and c) the Italian Telescopio Nazionale Galileo operated by the Fundación Galileo Galilei of the INAF (Istituto Nazionale di Astrofisica). All these facilities are located at the Spanish Roque de los Muchachos Observatory of the Instituto de Astrofísica de Canarias on the island of La Palma. This research has been carried out with telescope time awarded for the programme 128-MULTIPLE-16/15B. Also, during our analysis, we used the following databases: the SZ-Cluster Database operated by the Integrated Data and Operation Center (IDOC) at the IAS under contract with CNES and CNRS and the Sloan Digital Sky Survey (SDSS) DR14 database. Funding for the SDSS has been provided by the Alfred P. Sloan Foundation, the Participating Institutions, the National Aeronautics and Space Administration, the National Science Foundation, the U.S. Department of Energy, the Japanese Monbukagakusho, and the Max Planck Society. This work has been partially funded by the Spanish Ministry of Economy and Competitiveness (MINECO) under the projects ESP2013-48362-C2-1-P, AYA2014-60438-P and AYA2017-84185-P. AS and RB acknowledge financial support from the Spanish Ministry of Economy and Competitiveness (MINECO) under the Severo Ochoa Programmes SEV-2011-0187 and SEV-2015-0548. HL is funded by PUT1627 grant from the Estonian Research Council and by the European Structural Funds grant for the Centre of Excellence "Dark Matter in (Astro)particle Physics and Cosmology" TK133. Some of the results in this paper have been derived using the HEALPix (Górski et al. 2005) package.

References

Abell, G. O., Corwin, Jr., H. G., & Olowin, R. P. 1989, *ApJS*, 70, 1
 Aghanim, N., Hürler, G., Diego, J. M., et al. 2015, *A&A*, 580, A138
 Allen, S. W., Evrard, A. E., & Mantz, A. B. 2011, *ARA&A*, 49, 409
 Amodeo, S., Mei, S., Stanford, S. A., et al. 2018, *ApJ*, 853, 36
 Barrena, R., Streblyanska, A., Ferragamo, A., et al. 2018, *A&A*, 616, A42
 Bertin, E. & Arnouts, S. 1996, *A&AS*, 117, 393
 Bleem, L. E., Stalder, B., de Haan, T., et al. 2015, *ApJS*, 216, 27
 Boada, S., Hughes, J. P., Menanteau, F., et al. 2019, *ApJ*, 871, 188
 Buddendiek, A., Schrabback, T., Greer, C. H., et al. 2015, *MNRAS*, 450, 4248
 Burenin, R. A. 2017, *Astronomy Letters*, 43, 507
 Burenin, R. A., Bikmaev, I. F., Khamitov, I. M., et al. 2018, *Astronomy Letters*, 44, 297
 Chambers, K. C., Magnier, E. A., Metcalfe, N., et al. 2016, *arXiv e-prints*, arXiv:1612.05560
 Cutri, R. M., Wright, E. L., Conrow, T., et al. 2013, *Explanatory Supplement to the AllWISE Data Release Products*, Tech. rep.

De Propriis, R., Couch, W. J., Colless, M., et al. 2002, *MNRAS*, 329, 87
 Gladders, M. D. & Yee, H. K. C. 2000, *AJ*, 120, 2148
 Górski, K. M., Hivon, E., Banday, A. J., et al. 2005, *ApJ*, 622, 759
 Hambly, N. C., MacGillivray, H. T., Read, M. A., et al. 2001, *MNRAS*, 326, 1279
 Hasselfield, M., Hilton, M., Marriage, T. A., et al. 2013, *J. Cosmology Astropart. Phys.*, 7, 008
 Khatri, R. 2016, *A&A*, 592, A48
 Komatsu, E., Smith, K. M., Dunkley, J., et al. 2011, *ApJS*, 192, 18
 Monet, D. G., Levine, S. E., Canzian, B., et al. 2003, *AJ*, 125, 984
 Munari, E., Biviano, A., Borgani, S., Murante, G., & Fabjan, D. 2013, *MNRAS*, 430, 2638
 Perrott, Y. C., Olamaie, M., Rumsey, C., et al. 2015, *A&A*, 580, A95
 Piffaretti, R., Arnaud, M., Pratt, G. W., Pointecouteau, E., & Melin, J.-B. 2011, *A&A*, 534, A109
 Planck Collaboration I. 2014, *A&A*, 571, A1
 Planck Collaboration int. I. 2012, *A&A*, 543, A102
 Planck Collaboration int. XXVI. 2015, *A&A*, 582, A29
 Planck Collaboration int. XXXVI. 2016, *A&A*, 586, A139
 Planck Collaboration VI. 2018, *arXiv e-prints*, arXiv:1807.06209
 Planck Collaboration XI. 2014, *A&A*, 571, A11
 Planck Collaboration XXII. 2016, *A&A*, 594, A22
 Planck Collaboration XXIV. 2016, *A&A*, 594, A24
 Planck Collaboration XXIX. 2014, *A&A*, 571, A29
 Planck Collaboration XXVII. 2016, *A&A*, 594, A27
 Predehl, P., Andritschke, R., Böhringer, H., et al. 2010, in *Society of Photo-Optical Instrumentation Engineers (SPIE) Conference Series*, Vol. 7732, Proc. SPIE, 77320U
 Rykoff, E. S., Rozo, E., Busha, M. T., et al. 2014, *ApJ*, 785, 104
 Skrutskie, M. F., Cutri, R. M., Stiening, R., et al. 2006, *AJ*, 131, 1163
 Streblyanska, A., Aguado-Barahona, A. R., Ferragamo, A., et al. 2019, *A&A*
 Streblyanska, A., Barrena, R., Rubiño-Martín, J. A., et al. 2018, *A&A*, 617, A71
 Sunyaev, R. A. & Zeldovich, Y. B. 1972, *Comments on Astrophysics and Space Physics*, 4, 173
 van der Burg, R. F. J., Aussel, H., Pratt, G. W., et al. 2016, *A&A*, 587, A23
 Voges, W., Aschenbach, B., Boller, T., et al. 1999, *VizieR Online Data Catalog*, 9010
 Voges, W., Aschenbach, B., Boller, T., et al. 2000, *VizieR Online Data Catalog*, 9029
 Wen, Z. L. & Han, J. L. 2018, *MNRAS*, 481, 4158
 Wen, Z. L., Han, J. L., & Liu, F. S. 2012, *ApJS*, 199, 34
 Wright, E. L., Eisenhardt, P. R. M., Mainzer, A. K., et al. 2010, *AJ*, 140, 1868
 York, D. G., Adelman, J., Anderson, Jr., J. E., et al. 2000, *AJ*, 120, 1579
 Zaznobil, I. A., Burenin, R. A., Bikmaev, I. F., et al. 2019, *Astronomy Letters*, 45, 49
 Zehren, H., Schrabback, T., & van der Burg, R. F. J. 2019, *MNRAS*
 Zwicky, F. 1933, *Helvetica Physica Acta*, 6, 110

¹ Instituto de Astrofísica de Canarias, C/Vía Láctea s/n, E-38205 La Laguna, Tenerife, Spain
 e-mail: aaguado@iac.es

² Universidad de La Laguna, Departamento de Astrofísica, E-38206 La Laguna, Tenerife, Spain

³ University of KwaZulu-Natal, Westville Campus, Private Bag X54001, Durban 4000, South Africa

⁴ Tartu Observatory, University of Tartu, Observatooriumi 1, 61602, Tõravere, Estonia